Available online at www.springerlink.com

Acta Metall. Sin. (Engl. Lett.) Vol.26 No.3 pp. 271—276 June 2013

ACTA
METALLURGICA SINICA
(ENGLISH LETTERS)

Pitting Corrosion of 13Cr Steel in Oxygen-free Completion Fluids of Organic Salt

Lining XU†, Yao MENG, Yunguang SHI and Yan LIU

Key Laboratory for Environmental Fracture (MOE), Institute of Advanced Materials and Technology, University of Science and Technology Beijing, Beijing 100083, China

[Manuscript received 31 December 2012, in revised form 4 March 2013]

Corrosion behavior of 13Cr steel in oxygen-free completion fluids of the organic salt at 180 °C was studied. Cross-sectional morphologies of the corrosion products were observed by scanning electron microscopy. Energy dispersive spectrum (EDS) was used to study the element distribution of the corrosion product inside and outside the pits. The results show that the organic salt causes severe pitting corrosion of 13Cr steel. The width and depth of the pits increase simultaneously when the test duration prolongs, and potassium enriches inside the pits.

KEY WORDS: 13Cr steel; Pitting corrosion; Organic salt; Completion fluids

1. Introduction

Corrosion of tubular goods is a significant problem during the course of oil and gas exploitation[1]. The drilling and completion fluids are corrosive to casing and tubing, especially in deep and hot wells[2,3]. The completion fluids are utilized to balance the high formation pressure of deep well and to maintain borehole stability[4,5]. The basis of completion fluids is salt, and the environmentally-friendly organic salt is widely used[6,7].

Due to better corrosion resistance and lower cost compared with other stainless steels such as duplex stainless steel, 13Cr steel is widely used in oil and gas field[8]. Many investigations have been conducted on the corrosion of 13Cr steel in completion fluids environment, and the corrosion resistance at higher temperature (>150 °C) in the environment containing CO_2 is not good[9−14]. Yin *et al.*[15] found lots of corrosion micro-pits on the localized sites of corrosion product layers of 13Cr steel at 160 °C. Yevtushenko *et al.*[16] reported that the pitting corrosion can be inhibited by the formation of the $FeCO_3$ scales in protective long-time exposure experiments. Zhao *et al.*[17] reported that at 90 °C, the corrosion was controlled by activation, thereby 13Cr steel was susceptible to localized attack. While at 150 °C, a passive film mixing with corrosion products formed a cohere film, and the corrosion morphologies were uniform corrosion.

In all the above studies, CO_2 enhanced the corrosiveness of the completion fluids. The study on the corrosion of 13Cr steel in CO_2-free and oxygen-free completion fluids environment is still lacking. The aim of this work is to investigate the corrosion behavior of 13Cr stainless steel in pure organic salt at high temperature (180 °C).

2. Experimental

The chemical composition of the 13Cr steel is shown in Table 1. The test specimen was 50 mm× 10 mm×3 mm. All the specimens were subsequently ground with 360, 800 and 1200 grit silicon carbide paper, rinsed with deionized water and degreased in acetone. Before each test, the specimens were weighed with an analytical balance in an accuracy of 10^{-4} g.

The completion fluids consist of organic salt of Potassium. The molecular formula is $X_mR_n(COO)K$, where X is hetero atom; R is alkyl. The test solution was simulating completion fluids of deep well with the

† Corresponding author. Assoc. Prof., Ph.D.; Tel: +86 10 62333972; Fax: +86 10 62334410; E-mail address: xulining@ustb.edu.cn (Lining XU)

DOI: 10.1007/s40195-012-0283-1

Table 1 Chemical composition (wt.%) of 13Cr stainless steel

C	Cr	Mn	Si	P	S	V	Fe
0.027	12	0.22	0.30	0.014	0.0035	0.041	Bal.

density of 1.7 g/cm^3. The test solution was deoxygenated by bubbling N_2 for 8 h.

Corrosion tests were conducted in a 3 L autoclave to investigate corrosion rate and corrosion morphology. Weight loss experiments were conducted in accordance with ASTM G31. The test pressure (5 MPa) was achieved with pure N_2 at 180 °C. The test duration was 7, 15, 30 and 60 d. After the test, the specimens were evaluated by weight loss method. Energy dispersive X-ray spectroscopy (EDS, Kevex SuperDry), scanning electron microscopy (SEM, LEO-1450) analyses and X-ray photoelectron spectroscopy (XPS, AXIS ULTRA^{DLD}) were employed to analyze the composition and morphology of the corrosion products.

3. Results and Discussion

The weight loss of 13Cr in organic salt at 180 °C under different test durations is shown in Table 2.

Table 2 Weight loss of 13Cr stainless steel in different test durations

7 d	15 d	30 d	60 d
0.0630 g	0.1785 g	0.0824 g	0.4628 g

The weight loss was undulate with the increases of the test duration, and it may relate to the emergence and development of pitting corrosion.

Fig. 1(a) shows the original surface of 13Cr sample and Figs. 1(b)—(d) show the macroscopic morphologies of different test durations after corrosion in completion fluids of organic salt. As shown in Figs. 1(b)—(d), the sample surfaces were covered with tight, complete film without obvious sags. Organic salt particles precipitated from the test solution and covered the sample surface, forming a green film. This film covered the corrosion product on the steel surface. With the increase of test duration, particles on the sample surface grew up gradually, so did the thickness of the organic salt film. Fig. 2 shows the macroscopic mor-

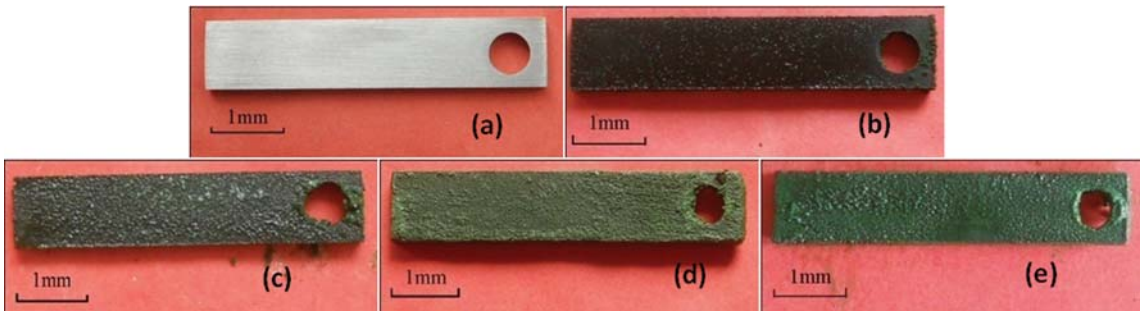

Fig. 1 Macroscopic morphologies of 13Cr stainless steel samples in different test durations: (a) before test; (b) 7 d; (c) 15 d; (d) 30 d; (e) 60 d

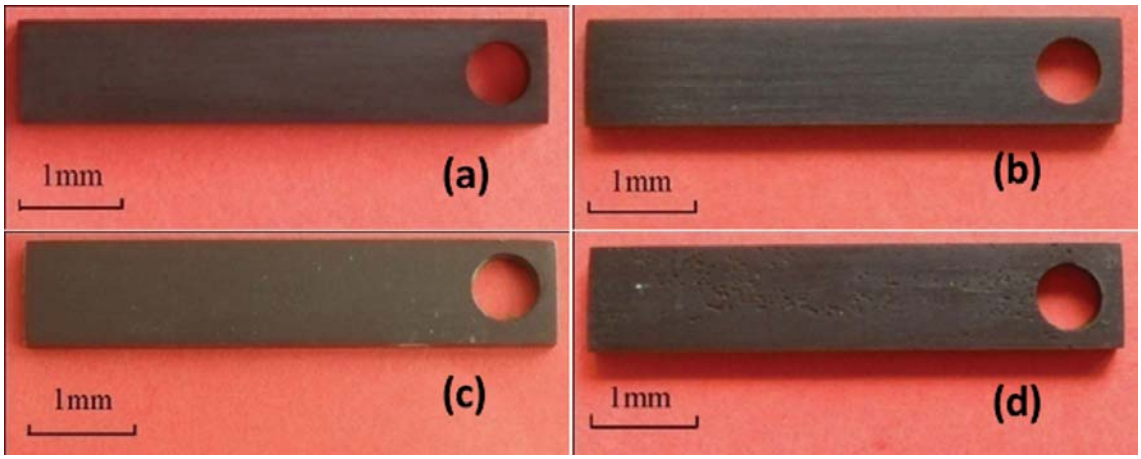

Fig. 2 Macroscopic morphologies of 13Cr stainless steel samples in different test durations after the removal of the corrosion product: (a) 7 d; (b) 15 d; (c) 30 d; (d) 60 d

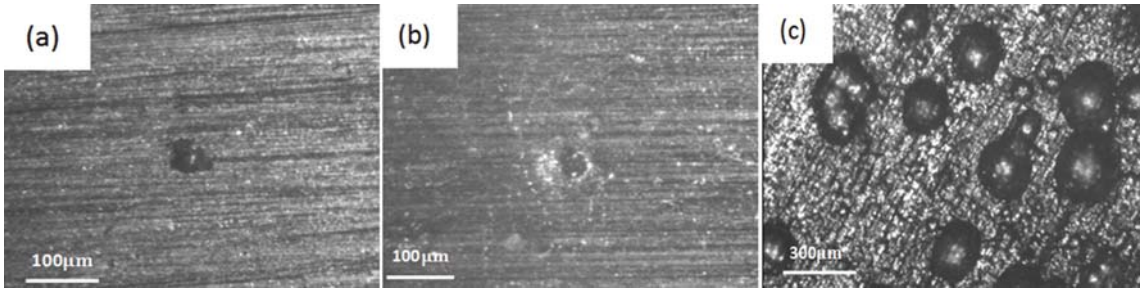

Fig. 3 SEM images of the pits after corrosion test of 15 d (a), 30 d (b) and 60 d (c)

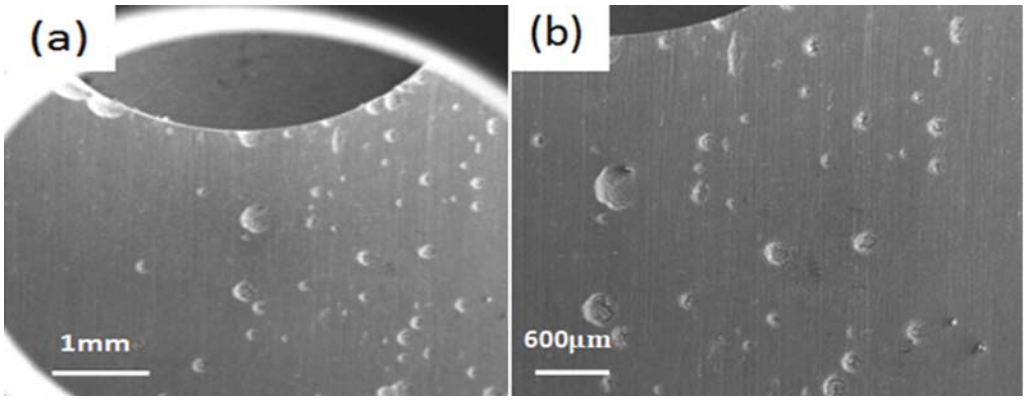

Fig. 4 SEM images of the surface of 13Cr stainless steel after 60 d corrosion test

Table 3 The average width and depth of the pits

Test duration (d)	Average width (μm)	Average depth (μm)
15	75	42.0
30	91	53.5
60	293	172.0

phologies of the samples after the removal of the corrosion product. As it was shown in Fig. 2, after the removal of the corrosion product and the organic salt film, the surface was no longer bright or flat like the original one (Fig. 1(a)). As exhibited in Fig. 2(d), there were many deep pits on the steel surface at the test duration of 60 d. It is clear that the small pits occurred after the corrosion of 15 d, and then gradually grew up with the test duration increasing, as shown in Fig. 3.

After the exposure of 7 d, pitting corrosion was not found on the surface of the samples. After the exposure of 15 and 30 d, several pits appeared on the sample surface, the size of the pits is around 70–90 μm as shown in Fig. 3. For longer exposure time (60 d), many pits appeared, and the average size was above 200 μm as shown in Fig. 4. Since the solution had been deoxygenated, the organic salt was probably the main cause of pitting corrosion. For the short time (7 d), pitting may be in gestation period and there was no apparent pit. After long time exposure, pits appeared and grew fast. Moreover, as shown in Table 3, the width of the pit is larger than its depth, which is much different from the deep and narrow pit happened on the 13Cr steel surface in CO_2 saturated brine[16].

According to Fig. 5, the pits in different stages (15 d, 30 d and 60 d) are all in the shape of hemisphere. Part of the corrosion product on the base metal near the pit falls off during the sample preparation process due to their poor adhesion, but the substance inside the pit remains perfect in shape and they protrude out of the interface between the base metal and corrosion product. Fig. 5 is the Electron Back Scattering Diffraction (EBSD) images of the pits, and different image contrasts represent different chemical compositions. As exhibited in the figure, the composition of the substance inside the pit (filler) was apparently different from those near the pit, and the filler was denser. With increasing test duration, the depth and width of the pits kept expanding and they remained in the shape of hemisphere.

Fig. 6 shows the enlarged figure of a pit formed after 15 d, and the corrosion product (zone A) and the filler (zone B) were analyzed by using EDS technique. The results are shown in Tables 4 and 5. There is much Fe, Cr and some K in zone A, which means the precipitates are the mixture of the corrosion product

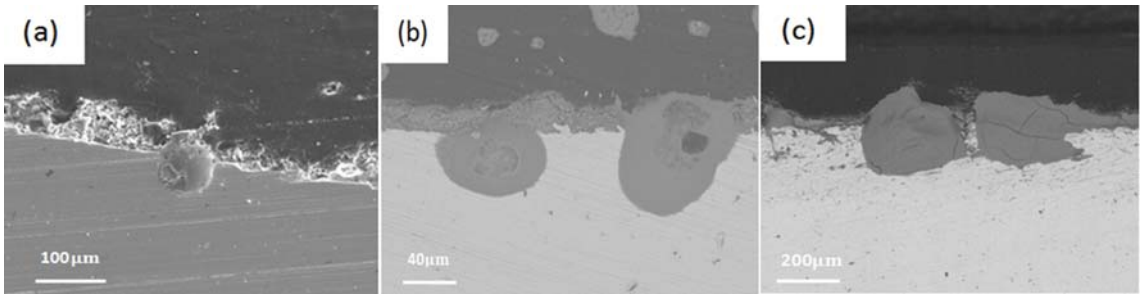

Fig. 5 Cross sectional morphologies of 13Cr stainless steel after corrosion test of 15 d (a), 30 d (b) and 60 d (c)

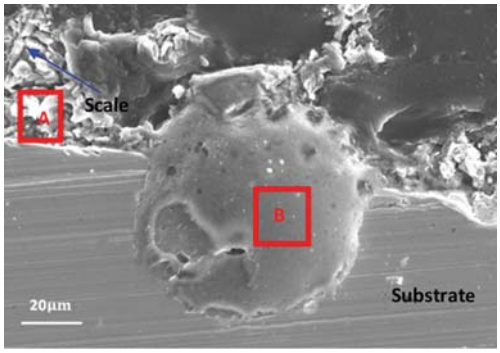

Fig. 6 Cross sectional morphology of a pit after 15 d corrosion test

Table 4 EDS results in zone A shown in Fig. 6 (wt.%)

O	P	K	Cr	Fe
19.50	5.86	9.98	19.57	42.39

Table 5 EDS results in zone B shown in Fig. 6 (wt.%)

O	P	K	Na	Fe
41.02	17.09	38.23	2.99	0.68

and the organic salt, and zone A appears to be loose and porous. Zone B contains little Fe but much K, meaning that the substance inside the pit is mainly organic salt. In order to reveal the element distribution of the filler, the area scan technique was used, as shown in Fig. 7, indicating the element distribution of the pit produced in the test of 15 d. As exhibited in the figures, filler of the pit contained little Fe and Cr, Much K and P, which were the main composition of the organic salt, were in the filler, and their distribution was uniform. Besides, the upper part of the filler, which protruded out of the base metal/corrosion

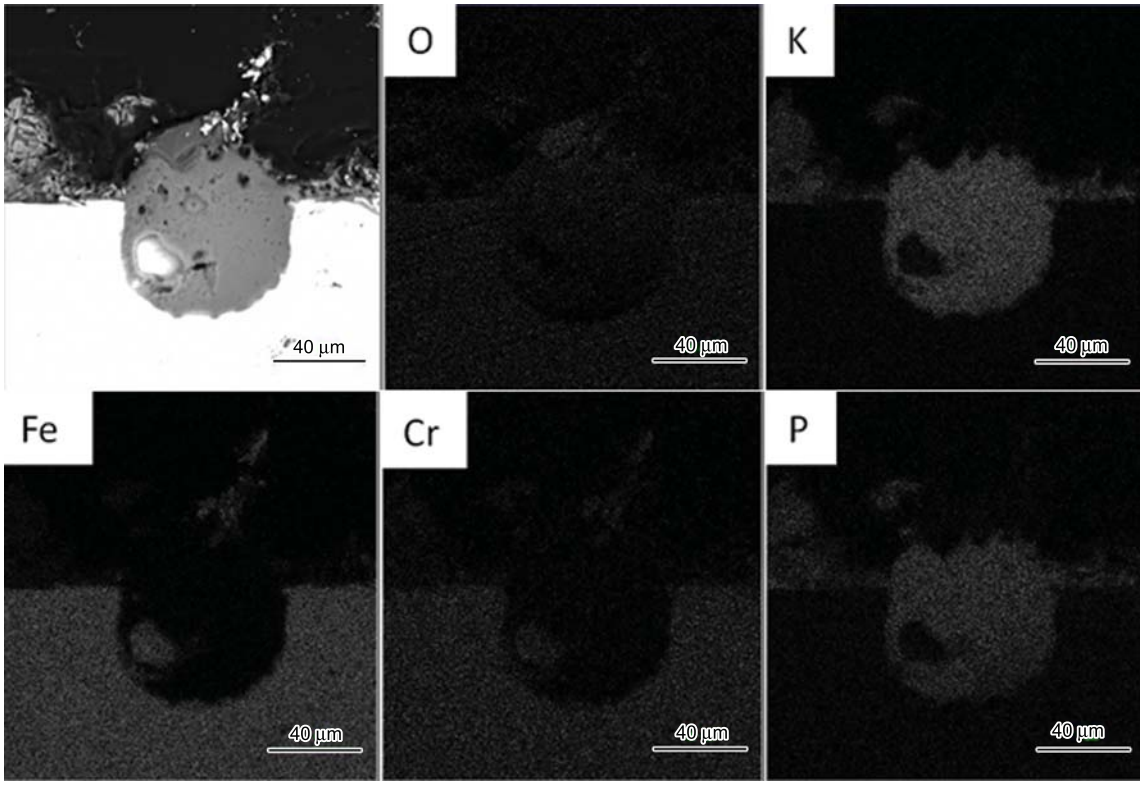

Fig. 7 Area scan EDS results of a pit on the 13Cr stainless steel after of 15 d corrosion test

Fig. 8 Schematic of the pits development

product interface, had the same composition as that inside the pit. As the ball-like filler was compact, it remained perfect with adjacent corrosion product peeled off. These results reveal that the character of 13Cr steel in oxygen-free organic salt environment was the hemisphere pit and the ball-like organic salt filler.

4. Discussion

According to the shape and size of the pits obtained under different test durations, pit development can be deduced, as shown in Fig. 8, the discussion is given briefly as follows:

The pitting corrosion of 13Cr steel in organic salt environment is caused by many factors. The organic salt particles from the solution are the main reason. The density of the test solution is high (1.7 g/cm^3), so the weight ratio of organic salt to water is as high as 200%. The organic salt particles generated in the solution will gather onto the surface of the metal. And the place that organic salt particles may become the nucleation site for the pit. In the environment with high temperature and high pressure (180 °C, 5 MPa), the pits grow very fast and cause serious pitting corrosion.

According to literatures, the pitting corrosion of the stainless steel usually follow occluded cell corrosion theory[18,19]. The depth of the pit kept increasing in a slender form as the time increases. Compared with the traditional pits, the ones occurred in the organic salt environment have their own characteristics. The width and depth of the pit increase at the same time, nearly at the same rate, forming the shape of half globular. Generally, pitting is related to the electro-chemical reactions, so the probable anodic and cathodic reaction of 13Cr steel in the organic salt solution without oxygen are discussed, as shown in the following equations:

Anodic reaction:

$$\mathrm{Fe} - 2\mathrm{e}^- = \mathrm{Fe}^{2+} \tag{1}$$

Cathodic reaction:

$$2\mathrm{RCOOK} + 2\mathrm{e}^- + 2\mathrm{H_2O} = 2\mathrm{RCOO}^- + 2\mathrm{KOH} + \mathrm{H_2} \tag{2}$$

The pH value of the original organic salt solution was 8.57, and the pH value become 9.60 after corrosion test and it is significantly higher. This phenomenon is in accordance with reaction (2). By providing chemical state information, XPS is the ideal tool to characterize the composition of the scale. Fig. 9 shows the high resolution XPS spectrogram of the scale. The

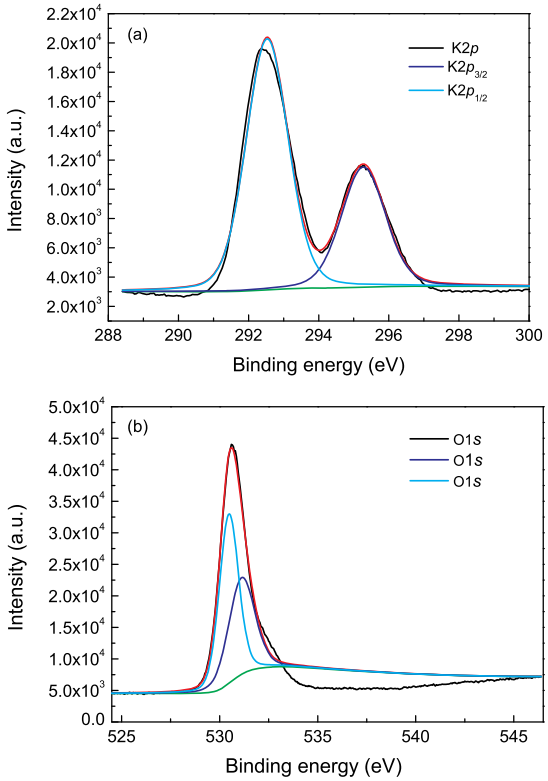

Fig. 9 XPS spectra and peak decomposition for K2p (a) and O1s (b) of the scale

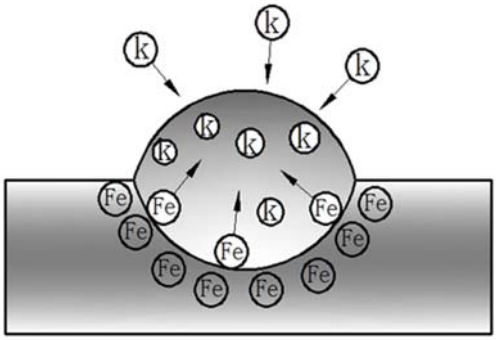

Fig. 10 Schematic of the mechanism of pitting corrosion

elements of interest are K and O. An examination of the K2p peaks reveals a K2$p_{3/2}$ peak at a binding energy of 295.27 eV and a K2$p_{1/2}$ peak at a binding energy of 292.53 eV, both corresponding to KOH. The O1s spectra can be divided into two peaks: the one near 531.12 eV is typical oxygen of KOH, and the other around 530.47 eV is probably associated with the Fe_2O_3 or Fe_3O_4.

Results indicate the enrichment of potassium inside the pits. If the potassium is in a form of ions, there will be a serious surplus of positive ions inside the pits. Fe^{2+} generated from the reaction (1) will be forced out of the pit under the influence of electric field. The environment with high temperature and high pressure (180 °C, 5 MPa) and high conductivity of solution in the pit caused by potassium enrichment

accelerate this process.

The probable pitting corrosion mechanism in oxygen-free organic salt environment is shown in Fig. 10. Ferrous corrosion product generated from the reaction (1) will be forced out of the pit, and Fe content inside the pit is much less than that around the pit. The product generated from anode reaction (Fe^{2+}) was quickly removed, resulting in the accelerated anodic reaction. Thus, the organic salt also caused the quick growth of pit even there is no oxygen involved in the corrosion process.

5. Conclusions

The pitting corrosion of 13Cr steel in completion fluids of the organic salt without oxygen has been investigated, and the results have been obtained as following. In oxygen-free organic salt environment with high temperature and high pressure (180 °C, 5 MPa), serious pitting corrosion occurred on 13Cr steel. The width and depth of the pits increase at the same time, which is not like the traditional deep and narrow pits. The enrichment of potassium is found inside the pit.

Acknowledgement

This work was supported by the National Science & Technology Pillar Program (No. 2012BAK13B04).

REFERENCES

[1] M.A. Simpson, S. Al-Reda, D. Foreman, J. Guzman and S. Aramco, in: the 40th Offshore Technology Conference, Houston, Texas, U. S., 4—7 May, 2009.
[2] J.D. Downs, in: the 17th Middle East Oil & Gas Show and Conference, Manama, Bahrain, 14–16 March, 2011.
[3] Z.Z. Yang, W. Tian and Q.R. Ma, Acta Metall. Sin. (Engl. Lett.) **21** (2008) 85.
[4] M.S. Ramsey, D.A. Texas, J.A. Shipp and B.J. Lang, in: SPE Annual Technology Conference, Denver, Colorado, 6–9 October, 1996.
[5] P. Guo, W. A. Gilchrist, J. Geoff Page, P. Wills and B. Atlas, in: the 43rd Annual Logging Symposium, Oiso, Japan, 4—7 June, 2002.
[6] D. Bungert, S. Maikranz, R. Sundermann, J. Downs, W. Benton and M.A. Dick, in: IADC/SPE Drilling Conference, New Orleans, Louisiana, U. S., 2—4 February, 2000.
[7] M. Brangetto, C. Pasturel and M. Gregoire, Drill. Contractor **63**(3) (2007) 108.
[8] M. Ueda and H. Takabe, in: NACE Corrosion Conference, Houston, Texas, U.S., 17—18 January, 1998.
[9] S. Hashizume, Y. Minami and Y. Ishizawa, in: NACE Corrosion Conference, Houston, Texas, U.S., 7—10 August , 1995.
[10] M.B. Kermani, G. Weighhill, T. Pendlington and G. Elliot, in: NACE Corrosion Conference, Houston, Texas, U.S., 7—10 August, 1995.
[11] R. Ebara, Mater. Sci. Eng. A **468–470** (2007) 109.
[12] R. Ebara, Proc. Eng. **2** (2010) 1297.
[13] S.I. Rokhlin, J.Y. Kim, H. Nagy and B. Zoofan, Eng. Fract. Mech. **62** (1999) 425.
[14] R.M. Schroeder and I.L. Muller, Mater. Corros. **60** (2009) 365.
[15] Z.F. Yin, X.Z. Wang, L. Liu, J.Q. Wu, and Y.Q. Zhang, J. Mater. Eng. Perform. **20** (2011) 1330.
[16] O. Yevtushenko, R. Babler and A. Pfennig, Mater. Corros. **63** (2010) 517.
[17] G.X. Zhao, M. Zheng, X.H. Lü, X.H. Dong and H.L. Li, Met. Mater. Int. **11** (2005) 135.
[18] R.C. Newman, Corrosion **57** (2001) 1030.
[19] G.S. Frankel, Electrochem. Soc. **145** (1998) 2186.